Click Here for Full Article

A model study of the vertically integrated transport variability through the Yucatan Channel: Role of Loop Current evolution and flow compensation around Cuba

Yuehua Lin,[1] Richard J. Greatbatch,[2] and Jinyu Sheng[1]

[1] The relationship between Loop Current intrusion in the Gulf of Mexico and vertically integrated transport variations through the Yucatan Channel is examined using models and the available observations. Transport in the model is found to be a minimum when the Loop Current intrudes strongly into the Gulf of Mexico, typically just before a ring is shed, and to be a maximum during the next growth phase in association with the buildup of warm water off the northwest coast of Cuba. We argue that the transport variations are part of a "compensation effect" in which transport variations through the Yucatan Channel are at least partly compensated by flow around Cuba. Numerical experiments show that the transport variations result from the interaction between the density anomalies associated with Loop Current intrusion and the variable bottom topography. The compensation effect is also shown to operate at shorter time scales (less than 30 days) in association with wind forcing.

1. Introduction

[2] The current system flowing through the Yucatan Channel and Straits of Florida (see Figure 1) is important because it is the major feeder for the Gulf Stream. Not only is this current system thought to be part of the wind-driven circulation of the subtropical gyre [*Schmitz et al.*, 1992], but it is also thought to be part of the upper limb of the North Atlantic meridional overturning circulation [*Schmitz and Richardson*, 1991] important for climate change. The Yucatan Channel has been the subject of an intensive monitoring study (Canek program) [*Ochoa et al.*, 2001; *Sheinbaum et al.*, 2002] using shipboard acoustic Doppler current profiler (ADCP) measurements, hydrographic/velocity surveys using conductivity-temperature-depth and lowered ADCP measurements, and a current meter mooring array. The Canek program was initiated in December 1996 and completed in June 2001. On the other hand, the Florida Current between Florida and the Bahamas has been monitored almost continuously since the early 1980s, beginning with the Subtropical Atlantic Climate Studies (STACS) program [*Schott and Zantopp*, 1985] and subsequently using submarine cables [*Larsen*, 1992; *Baringer and Larsen*, 2001]. More recently, monitoring of the Florida Current between Florida and the Bahamas has become an

essential part of the Research with Adaptive Particle Imaging Detectors/Meridional Overturning Circulation (RAPID/MOCHA) array for monitoring the North Atlantic meridional overturning circulation [*Cunningham et al.*, 2007; *Kanzow et al.*, 2007].

[3] A distinctive feature of the Gulf of Mexico is the intrusion of the Loop Current, connecting the Yucatan Channel with the Straits of Florida, and the associated ring shedding [see, e.g., *Hurlburt and Thompson*, 1980; *Oey et al.*, 2005]. The Loop Current can extend northward into the Gulf of Mexico, even as far as the Mississippi River delta and the Florida continental shelf [*Huh et al.*, 1981; *Wiseman and Dinnel*, 1988]. On the other hand, after shedding a ring, the Loop Current typically has a much more direct path from the Yucatan Channel to the Straits of Florida (port-to-port configuration). The mechanism supporting ring shedding has been widely studied, notably by *Hurlburt and Thompson* [1980], and more recently studied using the "momentum imbalance paradox" of *Pichevin and Nof* [1997] [see also *Nof and Pichevin*, 2001; *Nof*, 2005]. These studies showed that the ring shedding can be captured by a single-layer reduced gravity (1 1/2) layer model without the need to consider the interaction with the variable bottom topography.

[4] In the present paper we are not concerned with the mechanism of ring shedding but rather with the fluctuations in the vertically integrated transport that accompany Loop Current intrusion and ring shedding. Previous authors have concentrated on the connection between deep flow variations in the Yucatan Channel and ring shedding [e.g., *Maul et al.*, 1985; *Bunge et al.*, 2002; *Ezer et al.*, 2003; *Oey et al.*, 2005], while *Maul and Vukovich* [1993] used monthly mean

[1]Department of Oceanography, Dalhousie University, Halifax, Nova Scotia, Canada.
[2]Leibniz Institute of Marine Sciences at University of Kiel (IFM-GEOMAR), Kiel, Germany.
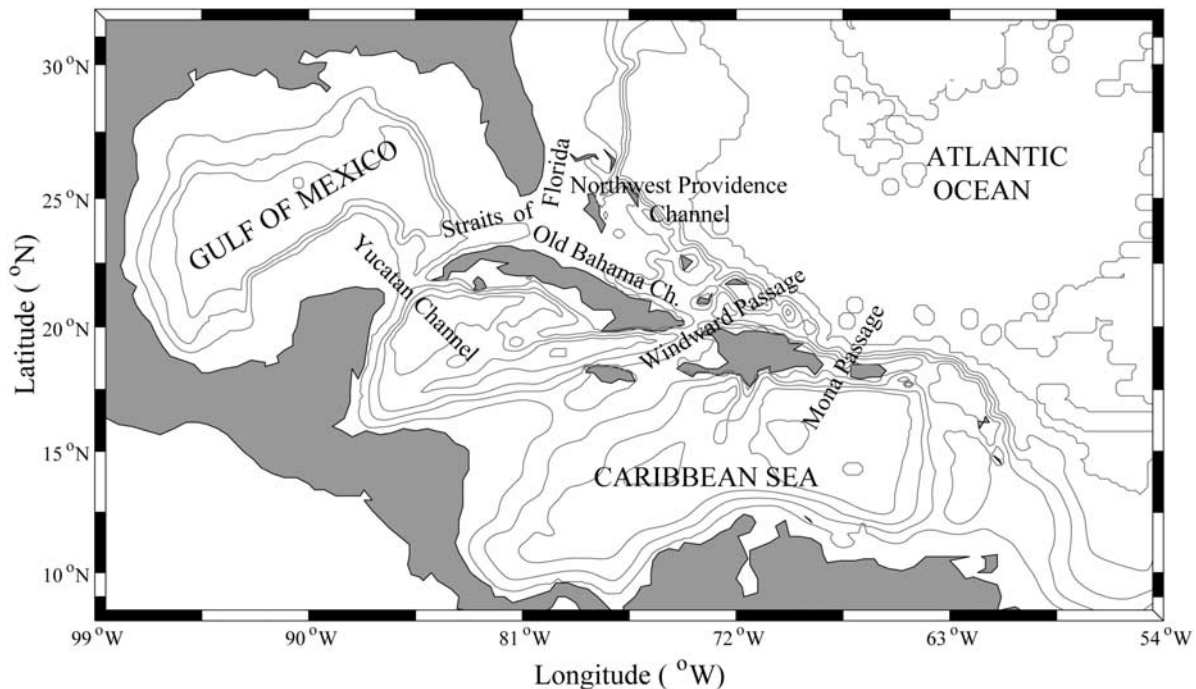
Figure 1. The model domain and major topographic features based on ETOPO5 (contour interval is 1000 m).

data to examine the relationship between variations in the Loop Current and the sea level difference between Cuba and Florida but found no clear relationship. There has also been much emphasis on the possible impact that changes in the flow conditions through the Yucatan Channel (e.g., flow velocity and the vorticity distribution) might play in preconditioning Loop Current intrusion and ring shedding [e.g., *Sheinbaum et al.*, 2002; *Ezer et al.*, 2003; *Oey et al.*, 2005; *Oey*, 2004]. Here the focus is the variation in the vertically integrated transport through the Yucatan Channel that accompanies Loop Current intrusion and ring shedding. We view these transport variations as being a consequence of Loop Current intrusion rather than the cause of the Loop Current intrusion itself (any possible feedback from the transport variations on the Loop Current intrusion is beyond the scope of this paper). Such fluctuations are clearly evident in the high-resolution model analyzed by *Cherubin et al.* [2005] and are also present in the 1/12° eddy-permitting Family of Linked Atlantic Model Experiments (FLAME) model of the Atlantic Ocean between 20°S and 70°N driven by climatological, seasonally varying forcing (see *Eden et al.* [2007] for a description of this model). Figure 2a shows time series of the vertically integrated transport through the Yucatan Channel and also between Florida and the Bahamas in the FLAME model, and Figure 2b shows the result of correlating the model sea surface height against the Yucatan Channel time series. The relationship between Loop Current intrusion and Yucatan Channel transport variability in the model is evident from the large negative correlation extending northward from the Yucatan Peninsula and the related region of positive correlation immediately to the west (correlations greater than 0.12 are significantly different from zero at the 99% level). It is also clear from the region of positive correlation around

Cuba that fluctuations in transport through the Yucatan Channel in the model are at least partly compensated by flow around Cuba, another issue we investigate in this paper.

[5] The arrangement of the paper is as follows. In section 2 the ocean model used in our study is described. Section 3 describes results from a specific experiment in which the relationship between Loop Current intrusion and transport variations through the Yucatan Channel is isolated. A more complete model run, including synoptic wind forcing, is then discussed in section 4. In section 5 we elucidate the mechanism connecting ring shedding and the transport variability using two diagnostic model runs. Section 6 then discusses the evidence for the compensation effect from the available observations, and section 7 provides a summary and discussion.

2. Model Setup and External Forcing

[6] The three-dimensional (3-D) numerical model used in this study is the primitive equation ocean circulation model CANDIE (the Canadian version of DieCAST model [*Sheng et al.*, 1998]). CANDIE has been successfully applied to address various modeling problems including the seasonal circulation in the northwestern Atlantic Ocean [*Sheng et al.*, 2001] and the general circulation over the western Caribbean Sea [*Sheng and Tang*, 2003, 2004; *Tang et al.*, 2006].

[7] The model domain covers the Intra-Americas Sea (99°W to 54°W, 8°N to 32°N, Figure 1) with a horizontal resolution in both latitude and longitude of 1/6°. The topographic data set used in the model is ETOPO5 (5-min gridded world elevations) from the National Geophysical Data Center. The temperature and salinity climatology is taken from the World Ocean Atlas Data 2001 of the
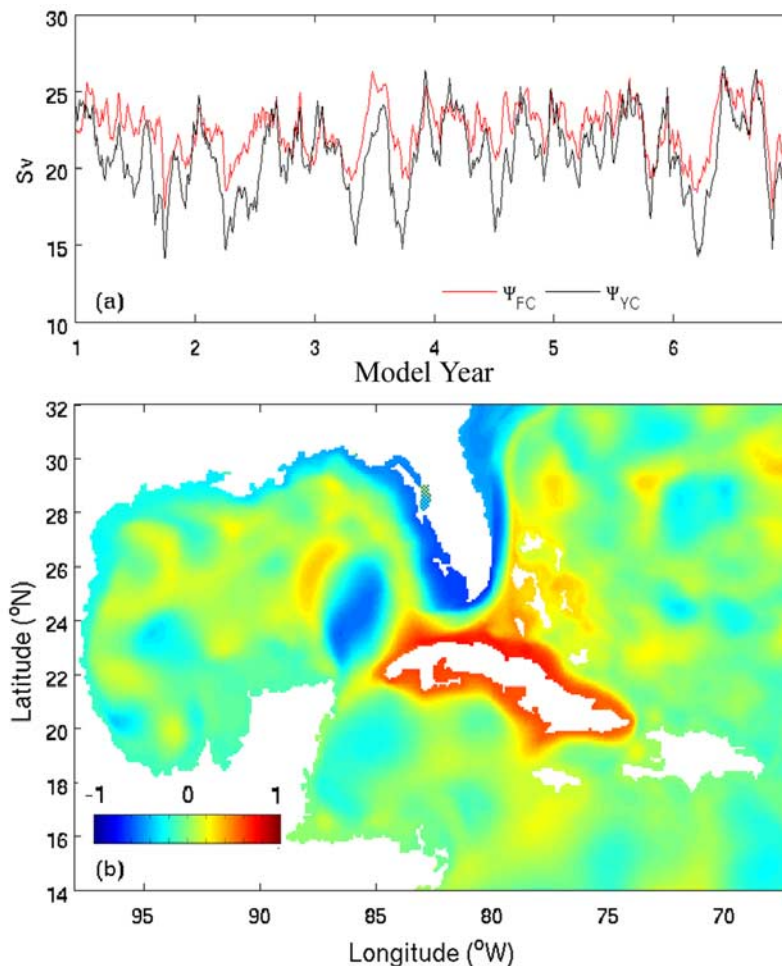
Figure 2. (a) Time series of the transport between Florida and the Bahamas (Ψ_{FC}) and through the Yucatan Channel (Ψ_{YC}) in the FLAME model, both positive northward. (b) Distribution of the correlation coefficient between the sea surface height anomalies and transport anomalies through the Yucatan Channel calculated from FLAME model results.

National Oceanographic Data Center in the United States and interpolated to the model grid.

[8] The model uses fourth-order numerics [*Dietrich*, 1998] and *Thuburn*'s [1996] flux limiter for the nonlinear advection terms. The subgrid scale mixing scheme of *Smagorinsky* [1963] is used for the horizontal eddy viscosity and diffusivity coefficients with the minimum value set to 15 m^2 s^{-1}, except where otherwise stated. The parameterization of *Large et al.* [1994] is used for the vertical eddy viscosity and diffusivity coefficients.

[9] The following boundary conditions are used. At lateral solid (or closed) boundaries, the normal flow, tangential stress, and normal fluxes of potential temperature and salinity are set to zero (free slip and insulating boundary conditions). Along the model open boundaries, the normal flow, temperature, and salinity fields are adjusted using a method similar to the adaptive open boundary conditions suggested by *Marchesiello et al.* [2001]. It first uses an explicit Orlanski radiation condition [*Orlanski*, 1976] to determine whether the open boundary is passive (outward propagation) or active (inward propagation). If the open boundary is passive, the model prognostic variables are radiated outward to allow any perturbation generated inside

the model domain to propagate outward as freely as possible. If the open boundary is active, the model prognostic variables at the open boundary are restored to the monthly mean climatologies at each z level with a time scale of 20 days. Furthermore, the depth-mean normal flows across the open boundaries are interpolated from the seasonally varying mean transports from the 1/12° version of the FLAME Atlantic Ocean model used to produce Figure 2.

[10] The results from four numerical experiments are described:

[11] 1. The control run (Exp-CR) model is forced by 6-hourly National Centers for Environmental Prediction (NCEP) wind fields from 1996 to 2001 (converted to wind stress using the formula of *Large and Pond* [1981]) and monthly mean surface heat flux [*da Silva et al.*, 1994] using the method of *Barnier et al.* [1995]. The model sea surface salinity is restored to the monthly mean climatology with a restoring time scale of 20 days. The model is initialized using January climatology for potential temperature and salinity.

[12] 2. The experiment Mean model is forced by annual mean (steady) wind stress and surface heat flux, and annual mean volume transports through the open boundaries are
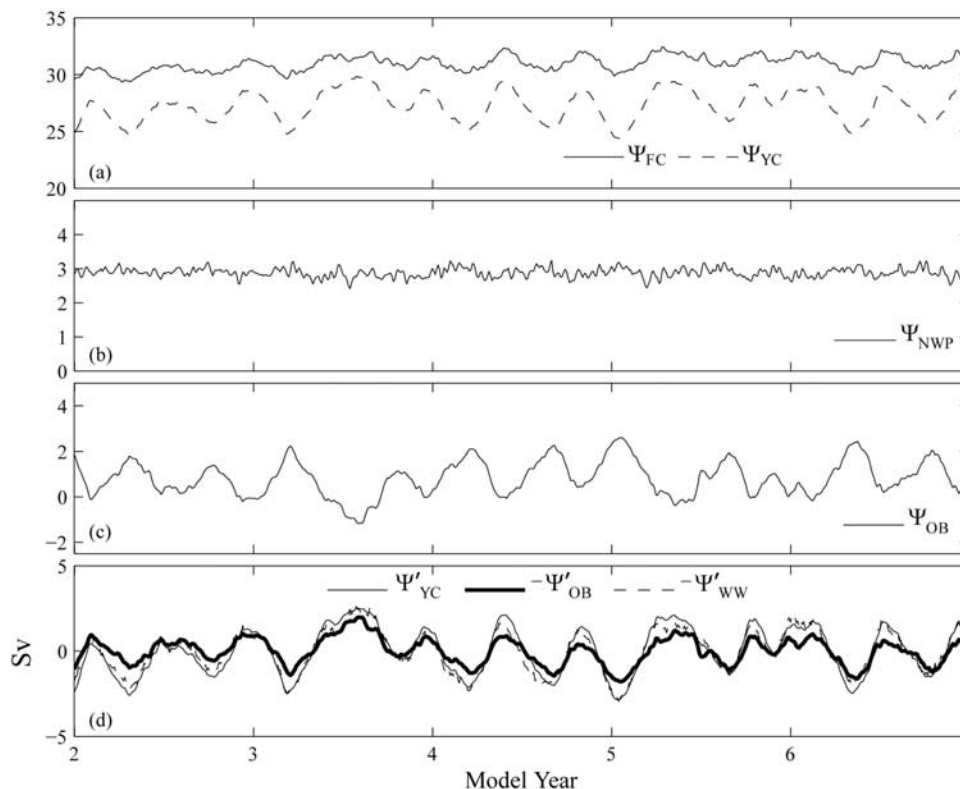
Figure 3. Time series of the model-calculated transports (3-day average) in experiment Mean from years 2 to 6 (a) between Florida and the Bahamas (Ψ_{FC}) and through the Yucatan Channel (Ψ_{YC}), (b) the transport through the Northwest Providence Channel (Ψ_{NWP}), and (c) the transport through the Old Bahama Channel (Ψ_{OB}). (d) Comparison between model-calculated transport anomalies (time mean removed) Ψ'_{YC}, $-\Psi'_{OB}$, and $-\Psi'_{WW}$ (Ψ_{WW} is the transport through the Windward Passage).

taken, as before, from the FLAME Atlantic Ocean model. The model sea surface salinity is restored to the annual mean climatology with a restoring time scale of 20 days. In this experiment, the background horizontal eddy viscosity and diffusivity coefficients are increased to 1.5×10^3 m^2 s^{-1} everywhere except for the region of the Gulf of Mexico and the adjacent area around Cuba in order to eliminate eddy activity outside the Gulf of Mexico. The model run in experiment Mean is purely prognostic.

[13] 3. In two diagnostic model runs, the time-independent potential temperature and salinity fields are specified in the model (the details are described in section 5). In these experiments there is no external forcing applied at the sea surface, and transports through open boundaries are set to zero. The model is integrated for 120 days to achieve a quasi steady state.

3. Experiment Mean: A Link Between Transport Variability Through the Yucatan Channel and Loop Current Intrusion Into the Gulf of Mexico

[14] We begin with experiment Mean. This experiment was integrated for 6 years, and the model results (3-day average) from day 360 to 2160 (i.e., from years 2 to 6) are used for analysis. Since the forcing in this experiment is time-independent, and eddy activity outside the Gulf of Mexico is eliminated by using a large horizontal eddy viscosity coefficient there, significant temporal variations

in the model are due entirely to the internal variability associated with the Loop Current intrusion and ring shedding. Figure 3a shows time series of the transport between Florida and the Bahamas (Ψ_{FC}) and through the Yucatan Channel (Ψ_{YC}) (both positive northward). The time mean transports are 31.0 and 27.3 Sv, respectively and are similar to the estimates given by *Johns et al.* [2002] based on their transport budget for the region (there is a slight linear trend in the transport time series due to model drift). As can be seen from Figure 3a, Ψ_{YC} exhibits quasiperiodic oscillations of a period around 5.5 months with the peak-to-peak transport difference reaching up to ~5 Sv. These quasiperiodic oscillations in transport are associated with quasiregular Loop Current ring shedding events in the model with a period of around 5.5 months. It is notable that although the influence of ring shedding can be seen in the transport of the Florida Current between Florida and the Bahamas, Ψ_{FC}, the transport variability is much weaker than that through the Yucatan Channel. It should be noted that transport between Florida and the Bahamas is free to vary in the model despite the fact that transport through the northern boundary of our model domain is fixed in this experiment (flow can pass north of the Bahamas, as happens in the FLAME model and as is implied by the region of positive correlation centered over the Bahamas in Figure 2b). It should also be noted that the difference in transport between the two time series plotted in Figure 3a compares well with
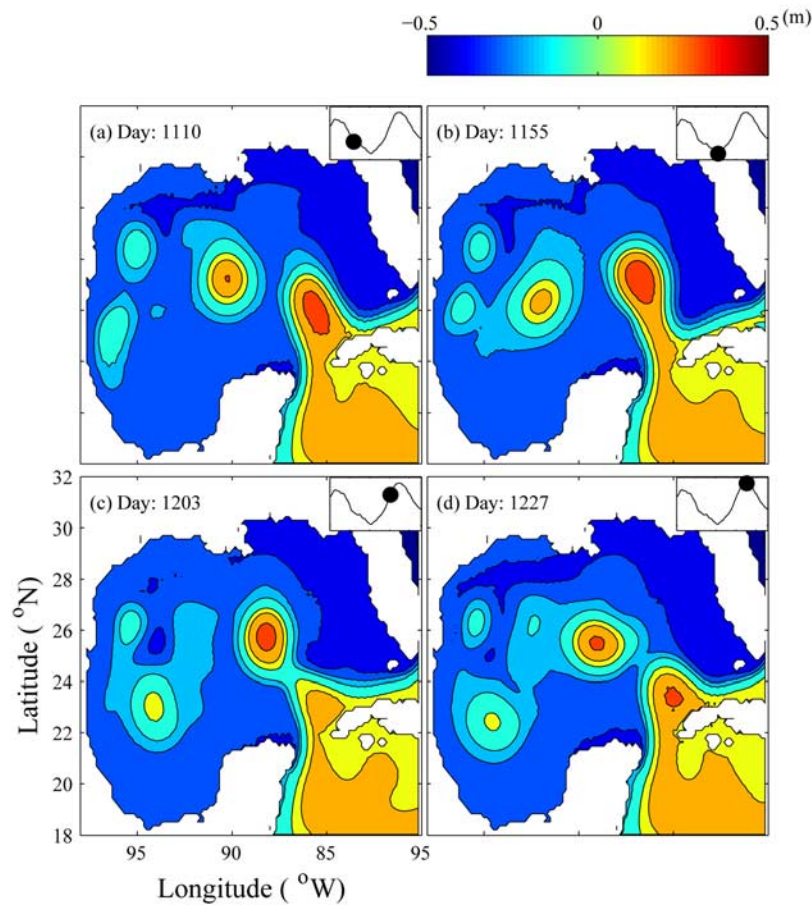
Figure 4. Snapshots of sea surface height fields (3-day average) produced by the model in experiment Mean and the corresponding transport variation through the Yucatan Channel (on the top right corner of Figures 4a–4d). Model time is marked by a solid dot on the time series of the transport through the Yucatan Channel.

the corresponding difference in transports found in the FLAME model and shown in Figure 2a.

[15] It is obvious from the geometry of the region (Figure 1) that if the transport through the Yucatan Channel and the transport of the Florida Current between Florida and the Bahamas do not vary together with the same amplitude, then there must be a significant compensating transport to the north of Cuba; in particular, through the Old Bahama and North Providence channels. The transport time series through these channels are shown in Figures 3b and 3c (transport is measured positive northwestward). It is clear that the main player in this experiment is the Old Bahama Channel, with relatively little transport variation taking place through the Northwest Providence Channel. Furthermore, from the comparison (Figure 3d) of the model-calculated transport anomalies (i.e., differences from the time mean) for Ψ'_{YC}, $-\Psi'_{OB}$, and $-\Psi'_{WW}$ (Ψ_{WW} represents the transport through the Windward Passage, positive northeastward), the temporal variability in Ψ_{YC} in the model is closely matched by southwestward transport anomalies through the Windward Passage, as well as southeastward transport anomalies through the Old Bahama Channel. It follows that at least in this experiment, transport variations in the Yucatan Channel are associated with anomalous transport around Cuba, connecting the Yucatan Channel with the Old Bahama Channel and the Windward Passage.

The above transport variations are an example of the "compensation effect" being introduced in this paper, whereby fluctuations in transport through the Yucatan Channel can be compensated, at least partly, by flow north of Cuba.

[16] The period of occurrence of the Loop Current ring shedding events in experiment Mean is about 5.5 months, which corresponds to the smaller of the two primary peaks in the distribution of observed periods noted by *Sturges and Leben* [2000]. Since the model external forcing is time-invariant in this experiment, the shedding period of ~5.5 months can be considered as the natural period of the ring shedding in the model. In the real ocean, the shedding frequency is influenced by many (external) factors such as the variability of forcing fields [*Sturges*, 1992] and eddies that propagate westward across the Caribbean Sea toward the Yucatan Channel [e.g., *Oey et al.*, 2003].

[17] Figure 4 shows the relationship between Loop Current intrusion/ring shedding and the Yucatan Channel transport, Ψ_{YC}, in the model. As can be seen, the Yucatan Channel transport decreases as the Loop Current intrudes into the Gulf of Mexico (Figure 4a), reaching a minimum (Figure 4b) when the Loop Current intrudes strongly into the gulf (Figure 4b) just as a ring starts to be shed. During the ring shedding, the transport starts to rise (Figure 4c) to reach a maximum soon after the ring is formed, at which

time a pool of anomalously warm water (anomalously high sea surface height) is found off the northwest coast of Cuba (Figure 4d). The transport variability documented here is consistent with the transport variability shown by *Cherubin et al.* [2005, Figure 3d] as well as with that in the FLAME model. The different phases of Loop Current intrusion and ring shedding are associated with density anomalies (departures from the time mean) in the model, and in section 5 we show that it is the interaction between these density anomalies and the underlying variable bottom topography that is responsible for the corresponding transport variations.

[18] Experiment Mean has been repeated using a smaller domain for which the eastern boundary cuts through Cuba. In this experiment, transport through the Yucatan Channel is fixed in time by the time-invariant transport specified on the eastern boundary south of Cuba. Loop Current intrusion and ring shedding still occur, as one expects from the model study of *Hurlburt and Thompson* [1980] and the theoretical study of *Pichevin and Nof* [1997]. However, the character of the Loop Current evolution is subtly different from that in Figure 4. In particular, the pool of warm water at the northwest corner of Cuba is a time-invariant feature, whereas in Figure 4, this feature varies as the transport varies. For example, in Figure 4, the Loop Current is strongly pinched to the north coast of Cuba when the transport is a minimum and the warm pool is absent (Figure 4b) but bulges away the coast when the transport is a maximum and the warm pool also reaches its maximum intensity (Figure 4d). As we show in section 5, the time variation of the warm pool is important for explaining the transport variations.

[19] In an additional experiment, the Windward and Mona passages were closed, with everything else remaining as in experiment Mean. Loop Current intrusion and ring shedding was found, as before, as well as the associated transport changes through the Yucatan Channel, with very little difference in behavior from experiment Mean. Since, however, the Windward and Mona passages are closed in this experiment, the transport variations connect south of the island of Puerto Rico rather than around Cuba, as in experiment Mean. The experiment shows that the Windward and Mona passages do not play a fundamental role in the dynamics of the transport changes, consistent with the analysis presented in section 5.

4. Control Run (Exp-CR)

[20] For a more general model setup, we now turn to the control run (Exp-CR). This experiment was integrated for 6 years, and the model results (3-day average) from days 360 to 2160 (i.e., from years 2 to 6) are used for analysis. We first describe the model validation and then move on to an analysis of the compensation effect in the model.

4.1. Model Validation

[21] In the model, the time-mean transport between Florida and the Bahamas, Ψ_{FC}, is 28.5 Sv, slightly less than the 32.3 ± 3.2 Sv estimated from the cable data [*Larsen*, 1992; *Baringer and Larsen*, 2001]. The time-mean transport through the Yucatan Channel, Ψ_{YC}, is 26.2 Sv, larger than the mean transport of 23.8 ± 1 Sv estimated from the Canek array [*Sheinbaum et al.*, 2002] but in keeping with the estimate for the Yucatan Channel transport given by *Johns*

et al. [2002] by closing the transport budget for the Antilles passages (the mean transport of 26.2 Sv is also consistent with the high-resolution model study of *Cherubin et al.* [2005]). The implied time-mean transport through the Old Bahama and Northwest Providence channels combined is 2.3 Sv and is similar to the observed estimates given by *Atkinson et al.* [1995] and *Leaman et al.* [1995]. We note that the time-mean transport through the Windward Passage into the Caribbean Sea in the model is about 5.4 Sv, which is underestimated compared to the estimate of 7 Sv made by *Johns et al.* [2002] but closer to the more recent estimate of 3.5 Sv given by *Johns et al.* [2008].

[22] There is a total of 10 eddy shedding events during the 5-year analysis period. The separation interval between shedding events varies between 5 and 8 months, which accords with the range of observed eddy separation intervals [e.g., *Vukovich*, 1995; *Sturges and Leben*, 2000]. Overall, our model exhibits similar behavior to that found in previous numerical studies [*Dietrich et al.*, 1997; *Murphy et al.*, 1999; *Oey et al.*, 2003].

[23] The observed vertical structure of the time-mean flow through the Yucatan Channel can be characterized as an intense northward flow into the Gulf of Mexico in the western upper part of the channel and relatively weaker and southward flow on the eastern upper and bottom layers (Figure 5a). A similar profile of the time-mean northward flow at the Yucatan Channel ($\sim$22°N) is produced by the model (Figure 5b). The time-mean temperature distribution at the same section based on the model results compares well with the observations during the Canek program, the isotherms being tilted to the surface in the western upper layer of the channel, as required by thermal wind to balance the intense northward flow. Furthermore, the location of the current maximum in the Yucatan Channel oscillates longitudinally associated with the Loop Current ring shedding events and the associated variations of the deep outflow (depth > 800 m) from the Gulf of Mexico, consistent with the *Bunge et al.* [2002] observations from Canek and the numerical simulations by *Ezer et al.* [2003] and *Cherubin et al.* [2005].

4.2. Compensation Effect in the Model

[24] Figure 6a shows model-calculated transport time series for the Florida Current between Florida and the Bahamas, Ψ_{FC}, and for the Yucatan Channel, Ψ_{YC}. The correlation coefficient at zero lag between the two time series is 0.89, significantly different from zero at the 99% level (Figure 7). (The corresponding correlation between the daily mean transport estimates from the cable data and the Canek data set is only 0.15, an issue discussed further in section 6.) Nevertheless, the two times series do not correspond exactly to each other, implying that some form of compensation effect must be operating in the model through the passageways north of Cuba. To examine this effect, Figures 6b and 6c show the transport time series from the model for the Northwest Providence (Ψ_{NWP}) and Old Bahama (Ψ_{OB}) channels. Correlation analysis (Figure 7) shows a significant negative correlation (0.85) between Ψ_{YC} and Ψ_{OB}, peaking near zero lag, indicative of the compensation effect, with only a very weak relationship between Ψ_{YC} and Ψ_{NWP}. It follows that in the model it is the transport variations through the Old Bahama Channel that contribute
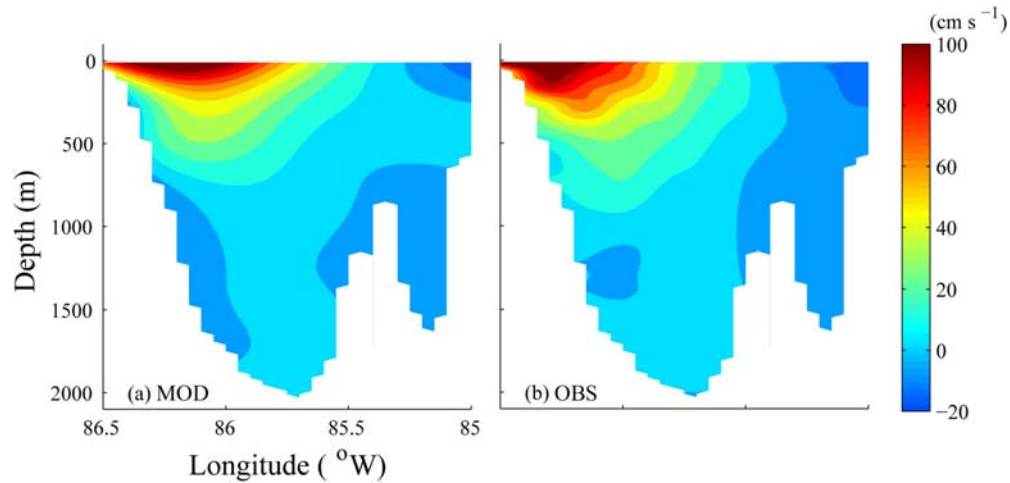
Figure 5. The time-mean northward normal velocity (cm s^{-1}) at the Yucatan Channel (a) observed by the Canek program from 13 July 2000 to 31 May 2001, and (b) produced by the model in Exp-CR from years 2 to 6. Model results are interpolated and extrapolated to the same data grid as observation data.
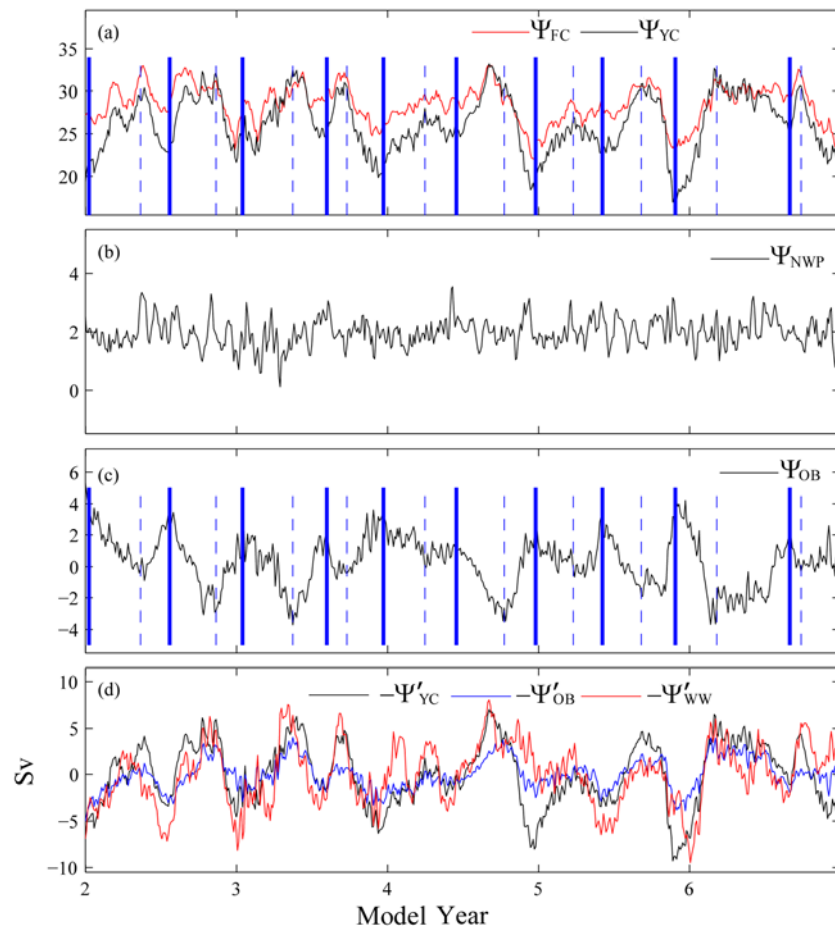

Figure 6. Time series of the model-calculated transports (3 day average) in Exp-CR from years 2 to 6 (a) between Florida and the Bahamas (Ψ_{FC}) and through the Yucatan Channel (Ψ_{YC}), (b) the transport through the Northwest Providence Channel (Ψ_{NWP}), and (c) the transport through the Old Bahama Channel (Ψ_{OB}). (d) Comparison between model-calculated transport anomalies (time mean removed) of Ψ'_{YC}, $-\Psi'_{OB}$, and $-\Psi'_{WW}$ (Ψ_{WW} presents the transport through the Windward Passage). The solid blue vertical lines mark the events corresponding to maxima of Ψ_{OB} and corresponding minima of Ψ_{YC} produced by the model in Exp-CR. The dashed vertical lines mark the events corresponding to minima of Ψ_{OB} and corresponding to maxima of Ψ_{YC}.
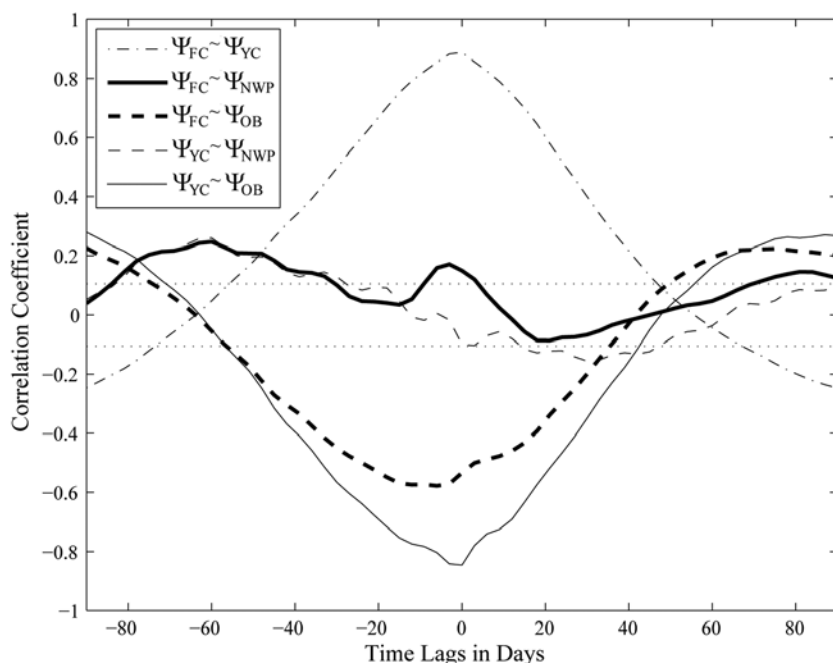
Figure 7. Correlation coefficients between transports of the Florida Current (Ψ_{FC}), the Yucatan Current (Ψ_{YC}), the flow through the Northwest Providence Channel (Ψ_{NWP}), and the flow through the Old Bahama Channel (Ψ_{OB}) calculated from model results (3-day average) in Exp-CR from years 2 to 6. Correlations outside the horizontal dotted lines are significantly different from zero at the 99% level.

to the compensation effect, with relatively little role for the Northwest Providence Channel, the same as we found when discussing experiment Mean in section 3. A comparison of the model-calculated transport anomalies (i.e., differences from the time mean) for Ψ'_{YC}, $-\Psi'_{OB}$, and $-\Psi'_{WW}$ is shown in Figure 6d. There is clearly a close relationship between all three time series. In particular, when Ψ_{YC} increases, there is a corresponding increase in the southeastward flow through the Old Bahama Channel and also increased southwestward flow through the Windward Passage, implying an anomalous clockwise circulation around Cuba, with the opposite situation applying when Ψ_{YC} is decreased, exactly as we found in experiment Mean.

[25] The connection between the large transport events in Figure 6 and the Loop Current intrusion is shown in Figures 8 and 9. shows the model sea surface height for all the events marked by the solid blue vertical lines in Figure 6 corresponding roughly to maxima in the northwestward transport through the Old Bahama Channel and corresponding minima in the northward transport through the Yucatan Channel. In each case, we see that the Loop Current intrudes strongly into the Gulf of Mexico, while at the same time it is pinched close to the northwest coast of Cuba, as in Figure 4b. Figure 9, on the other hand, shows the sea surface height corresponding roughly to minima (maxima) in the northwestward (northward) transport of the Old Bahama (Yucatan) Channel. This time we see the pool of warm water off the northwest coast of Cuba and an associated bulging of the Loop Current away from the coast but no deep intrusion into the gulf as in Figure 8. A comparison with Figures 4b and 4d shows the same features in the sea surface height in association with the minima and maxima in northward transport through the Yucatan Channel in experiment Mean. It is also interesting that in

Figures 8 and 9 we can see the presence of Caribbean eddies that squeeze through the Yucatan Channel (e.g., at day 1071 in Figure 8, and days 855, 1359, and 1866 in Figure 9).

[26] We have also calculated the distribution of correlation coefficients between the model sea surface height anomalies and anomalies of the model-calculated transport through the Old Bahama Channel (positive northwestward). The result is shown in Figure 10a and is reassuringly similar to the correlation map computed using FLAME model output, based on Yucatan Channel transport (note the sign change) and shown in Figure 2b. The presence of flow compensation around Cuba is clearly evident, as implied by the high negative correlation all around Cuba. The connection between Loop Current intrusion and the transport variability is indicated by the elongated region of large positive anomaly to the north of the Yucatan Peninsula and the northward bulge in the region of negative correlation off the northwest coast of Cuba.

[27] Flow compensation around Cuba is also a feature of the model results at higher frequency. (It should be noted that our model is driven by 6 hourly wind stress computed from NCEP wind fields.) Using model output that has been high-pass filtered with a cutoff time scale of 30 days, the correlation at zero lag between the northward transport through the Yucatan Channel and the northwestward transport through the Old Bahama Channel is -0.63 and is significantly different from zero at the 99% level. The amplitude of the high-frequency transport anomalies produced by the model varies from 0.5 to 2 Sv. Figure 10b shows the correlation of model sea surface height anomalies with northwestward transport anomalies through the Old Bahama Channel, again both high-pass filtered with a cutoff of 30 days. The pattern is quite different from that in Figure 10a, indicating that quite different dynamics are
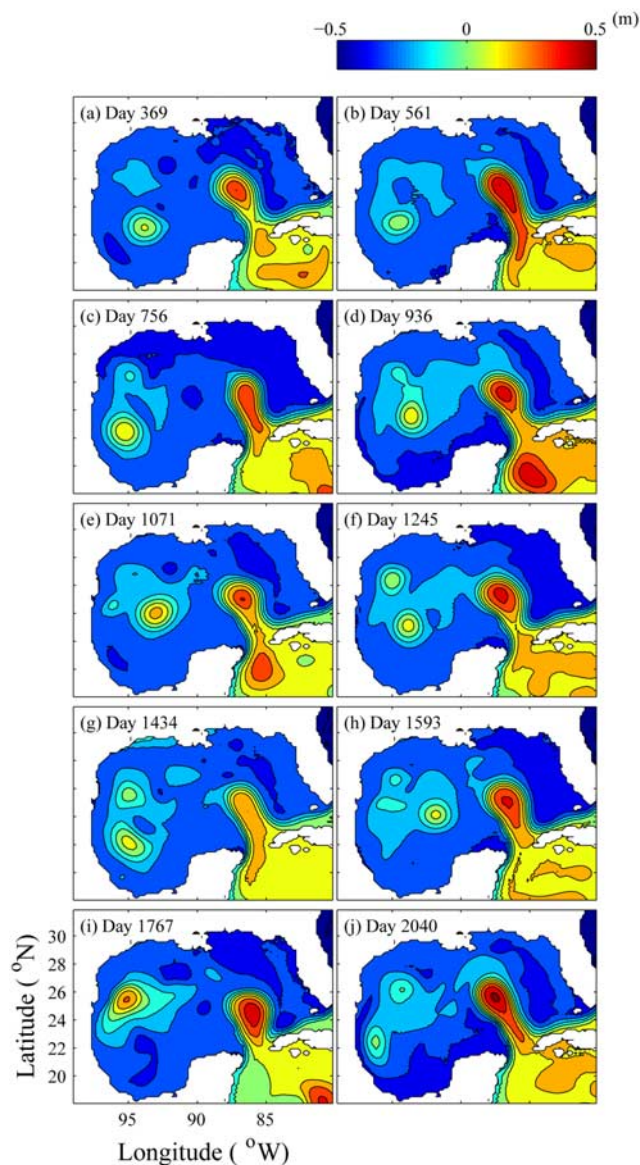
Figure 8. Snapshots of sea surface height fields (3-day average) for all the events marked by the solid blue vertical lines in Figure 6 produced by the model in Exp-CR.

held time-independent and the model otherwise has no forcing. In particular, the model is run in diagnostic mode using pseudohydrography constructed by adding potential temperature and salinity anomaly fields extracted from experiment Mean to the horizontal average of the annual mean climatology for the whole model domain. Surface forcing and transports through the model open boundaries are set to zero. The bottom friction and horizontal eddy viscosity (for momentum) are set to zero. Instead, a simple linear friction in the horizontal momentum equations is used at each level, i.e., a term in vector notation, $-\varepsilon(u, v)$, where ε corresponds to a time scale of 15 days (i.e., $1/\varepsilon = 15$ days) and has no vertical dependence. The use of a linear friction eliminates the possibility that rectification effects from the friction term can drive vertically integrated transport.

[29] The model is then integrated to reach a quasi steady state. In the first run, the model uses potential temperature and salinity anomalies taken from day 1155 in experiment
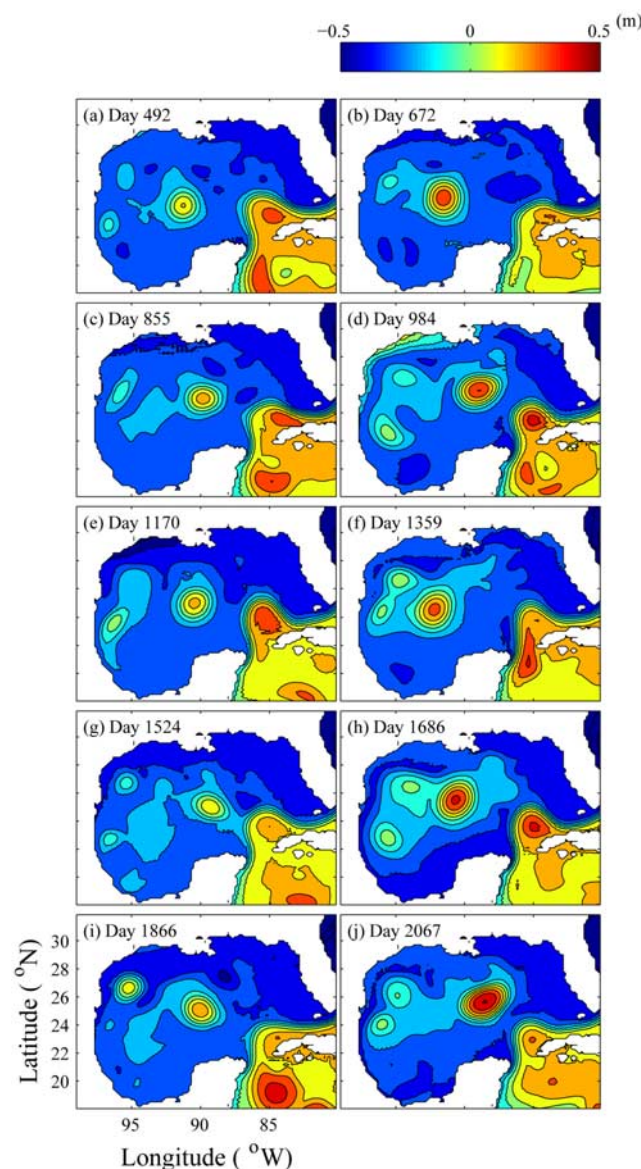
operating. In fact, at these high frequencies it is wind forcing that is important, the transport through the Old Bahama Channel being highly correlated with the along-channel wind stress. The influence of wind forcing is evident from Figure 10b with sea level anomalies of opposite sign on the north and south coast of Cuba indicative of Ekman divergence and convergence, respectively, in association with a westward wind stress.

5. Diagnostic Model Results: Mechanism by Which Loop Current Intrusion Affects Transport Variations at the Yucatan Channel

[28] To understand the dynamics responsible for the transport fluctuations through the Yucatan Channel, we have run the model in diagnostic mode in which the model potential temperature and salinity fields are specified and

Figure 9. Snapshots of sea surface height fields (3-day average) for all the events marked by the dashed vertical lines in Figure 6 produced by the model in Exp-CR.
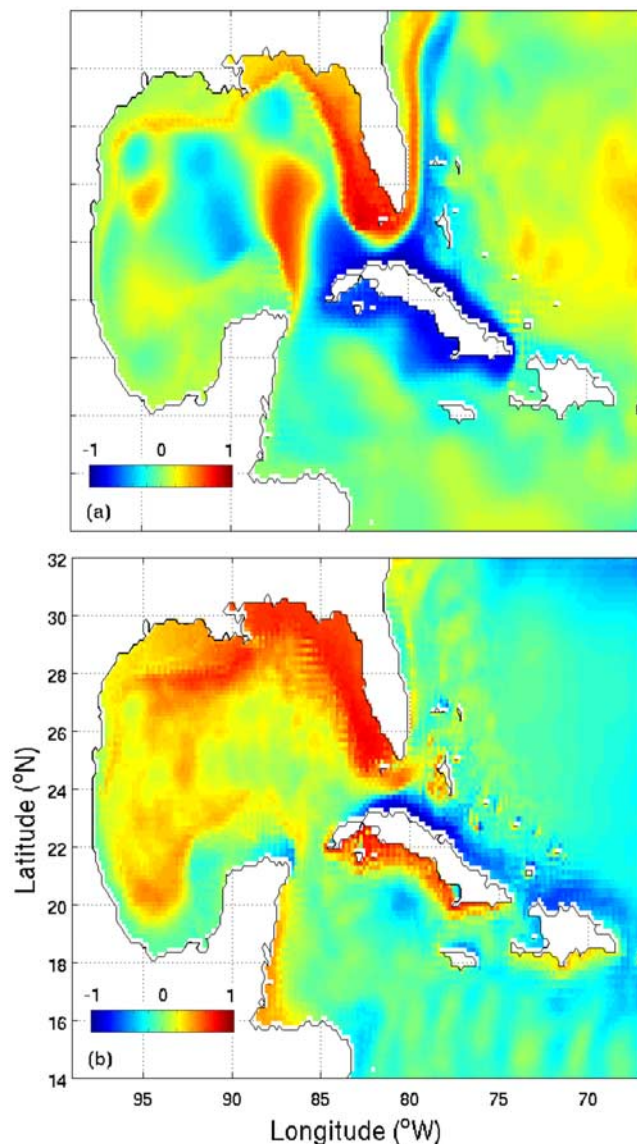
Figure 10. (a) Distribution of correlation coefficients between the sea surface height anomalies and transport anomalies through the Old Bahama Channel calculated from model results (3-day average) in Exp-CR from years 2 to 6. (b) Same as Figure 10a but for 30-day high-pass-filtered results.

Loop Current intrusion and ring shedding can be understood as the result of the interaction of the density anomalies and the underlying variable bottom topography.

[30] To identify the precise mechanism, we note that a feature of the geometry in this area is that the water depth in the Old Bahama Channel, and in the Straits of Florida between Florida and Cuba, is much less than that in the Yucatan Channel and the Gulf of Mexico to the west and in the North Atlantic Ocean to the east. As a consequence, pressure differences across the ridge connecting Florida and Cuba can affect the transport through the Straits of Florida between Cuba and Florida, and hence Ψ_{YC} by volume conservation, by means of the form drag effect. To illustrate the form drag effect, we consider the vertically integrated zonal momentum balance:

$$-fV = -\frac{1}{\rho_o}\frac{\partial}{\partial x}\int_{-H}^{o} p\,dz + \frac{1}{\rho_o}p_b H_x - \epsilon U,$$

where (U, V) is the vertically integrated transport vector, H is the water depth, p is the pressure perturbation from the undisturbed state, and p_b is the value of p at the bottom (corresponding to the bottom pressure). The second term on the right-hand side is the topographic form drag term associated with pressure differences across topographic ridges [see, e.g., *Hughes and de Cuevas*, 2001]. We use this equation to interpret the results from the diagnostic model. Integrating zonally across the model domain along a line of latitude passing between Florida and Cuba (i.e., passing through the Straits of Florida), the first term on the right-hand side goes to zero (it is zero at the western end of the section where the water depth, H, on the western side of the Gulf of Mexico goes to zero; and it is zero at the eastern end of the section where the transport variability is zero). Likewise, because no transport is allowed to pass through
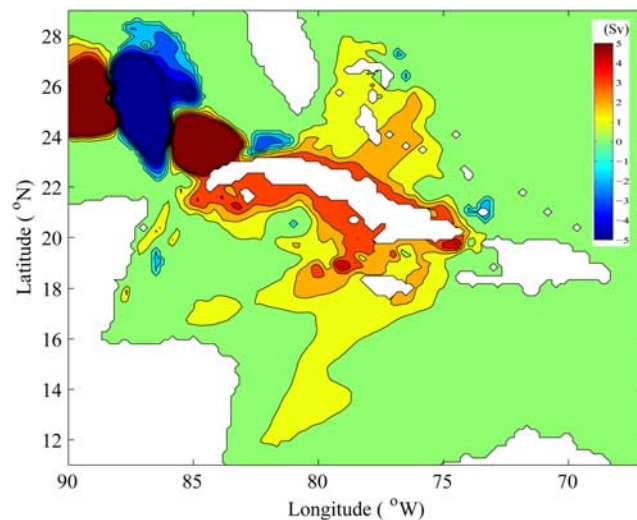
Mean, associated with a minimum of Ψ_{YC}, and in the second run, the model uses potential temperature and salinity anomalies from day 1230, associated with a maximum of Ψ_{YC} (see Figure 4). The first/second model run gives a cyclonic/anticyclonic circulation around Cuba (and hence a southward/northward transport anomaly through the Yucatan Channel). The volume transport stream function difference, the second run minus the first run, is shown in Figure 11. There is 3.8 Sv transport difference generated for Ψ_{YC}, comparable to the peak-to-peak transport difference found in experiment Mean. Of this 3.8 Sv, 2.5 Sv is associated with compensating flow through the Old Bahama Channel with the remaining 1.3 Sv circulating round and through the Bahama Island archipelago. Importantly, the results show that the compensation effect associated with

Figure 11. Differences in volume transport stream functions (color shading) between two diagnostic runs (in the steady state) driven by potential temperature and salinity anomalies extracted from model results in experiment Mean at day 1155 (corresponding to a minimum in transports through the Yucatan Channel) and day 1230 (corresponding to a maximum in transports through the Yucatan Channel).
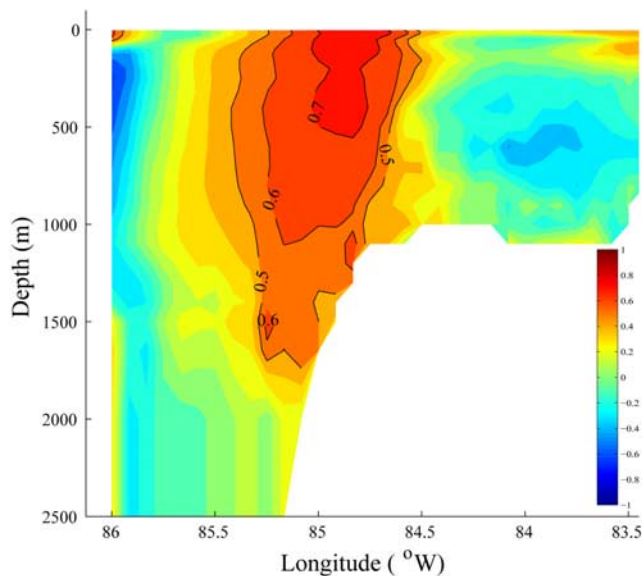
Figure 12. The vertical distribution of correlation coefficients along a transect at 23.9°N (the Straits of Florida between Florida and Cuba), between the model-calculated potential temperature field and the transport through the Yucatan Channel (positive northward) calculated from model results (3-day average) in experiment Mean from years 2 to 6.

the boundaries of the diagnostic model, the net northward transport across the line of latitude (the zonal integral of the term on the left-hand side) is also zero, leaving a balance between the friction term and the topographic form drag. (Note that the argument is unchanged if the line of latitude is blocked by islands and also if the line of integration is curved in order to follow a water-only path.)

[31] To illustrate the form drag mechanism, Figure 12 shows the correlation between the temperature field along 23.9°N, at the Gulf of Mexico entrance to the Straits of Florida, and Ψ_{YC} in experiment Mean. It can be seen that increased Ψ_{YC} is associated with warmer (lighter) water over the slope (this is the warm pool near the northwest coast of Cuba noted when discussing Figure 4d). By contrast, the hydrographic conditions on the topographic slope east of the Bahama Islands do not change in experiment Mean in relation to Yucatan Channel transport variability. As a consequence, in the run with the diagnostic model corresponding to a maximum in Ψ_{YC}, the bottom pressure is lower on the Gulf of Mexico side of the ridge, where the water is anomalously warm, than on the Bahamas side. The resulting pressure difference across the ridge then drives enhanced westward transport through the Straits of Florida by the form drag effect which, because of volume conservation, leads to the increased Ψ_{YC}.

[32] It is interesting that the transport difference shown in Figure 11 mirrors quite closely the features seen in the sea surface height pattern implied by Figure 10a. In particular, we can see the (negative) transport anomaly associated with the elongated feature to the north of the Yucatan Peninsula and, importantly, the (positive) transport anomaly off the northwest coast of Cuba. When the transport through the Yucatan Channel is enhanced, the latter feature is associated

with the pool of warm water off the northwest coast of Cuba, while the former feature indicates that when transport through the Yucatan Channel is enhanced, the deep intrusion by the Loop Current into the gulf is absent.

[33] We argue, therefore, that it is the interaction between the Loop Current intrusion and the sloping topography at the Gulf of Mexico entrance to the Straits of Florida that is responsible for the link between Yucatan/Old Bahama Channel transport variability and the Loop Current intrusion and ring shedding. In particular, the evolution of the Loop Current, as it intrudes into the Gulf of Mexico, leads both to the pinching of the flow to the northwest of Cuba, as in Figure 4b, and the expansion of the warm pool northwest of Cuba, as in Figure 4d. It is the density anomalies associated with the fluctuations in the warm pool that, through interaction with the sloping bottom topography, drive the transport variations. This conclusion is consistent with the two additional experiments described in section 3. In one, the Windward and Mona passages were closed, yet the transport variations were found as before. In the other, the transport through the Yucatan Channel was specified to be time-invariant by the model setup, and the warm pool northwest of Cuba became a steady, time-invariant feature of the model results.

6. Evidence for the Compensation Effect From Observations

[34] Two oceanographic data sets are of particular importance. The first is the daily mean transport of the Florida Current inferred from voltage differences across the Florida-Bahamas submarine cable at 27°N [*Baringer and Larsen*, 2001]. The second is the set of daily mean transport estimates from the 2-year observation array in the Yucatan Current during the Canek program [*Ochoa et al.*, 2001; *Bunge et al.*, 2002; *Sheinbaum et al.*, 2002; *Candela et al.*, 2003; *Abascal et al.*, 2003]. The data come from two periods: 10 September 1999 to 15 June 2000 and 13 July 2000 to 31 May 2001. For comparison, the observed transport estimates during the period 13 July 2000 to 31 May 2001 (when both observational data sets are available simultaneously) are shown in Figure 13. During this period, the cable-estimated transport of the Florida Current varied between 22.7 and 39.6 Sv and the Canek estimates of the Yucatan Channel transport between 12.8 and 31.7 Sv. Although there are events common to both time series (e.g., during March 2001) a visual inspection suggests that there is no clear relationship between the measured transport estimates. Indeed, the correlation at zero lag is only 0.15. As noted in section 4, the relationship between the two transport time series is very much stronger in the model (correlation at zero lag of 0.89). It should be noted, however, that we have less than 1 year of data with which to make the comparison, which is not long enough to properly access the impact of Loop Current intrusion in the two transport times series, whereas the Loop Current intrusion effect dominates the transport variability in the model. (In an attempt to access the correlation at low frequency, we have low-pass filtered both the Canek and cable transport time series with a cutoff of 120 days. The correlation between the two time series then rises to 0.5 and is more in keeping with the model. However, given the
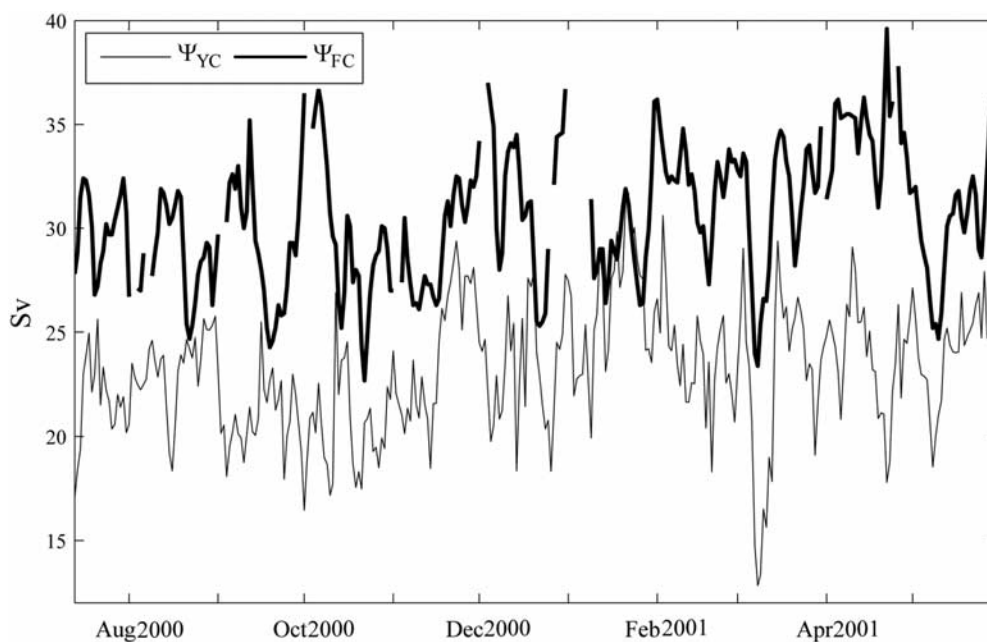
Figure 13. Time series of transports of the Florida Current from the cable data (Ψ_{FC}, thick lines) and through the Yucatan Channel based on the Canek program (Ψ_{YC}, thin line) from 13 July 2000 to 31 May 2001.

shortness of the time series we can use for the comparison, one cannot draw a firm conclusion.) In addition, in the model we are lacking transport variability on daily time scales through the boundary to the north of Straits of Florida due to the specification of a seasonally only varying transport time series taken from the FLAME model (see section 2). Nevertheless, if the transport estimates from the cable and Canek data sets are accurate, then in reality the compensation effect must operate to a much greater extent than we have found in the model. Of course, the low correlation between the Canek- and cable-estimated daily transport estimates could be because of data problems. For example, the mean transport through the Yucatan Channel from the Canek data set is 23.8 ± 1 Sv, as given by *Sheinbaum et al.* [2002], is considerably less than the 32.3 ± 3.2 Sv for the Florida Current between Florida and the Bahamas given by *Baringer and Larsen* [2001] and verified over many years against mooring observations (e.g., the STACS program [*Schott and Zantopp*, 1985]). The difference of more than 8 Sv is roughly double the transport estimated for the passages north of Cuba by *Atkinson et al.* [1995] and *Leaman et al.* [1995] [see also *Johns et al.*, 2002]. It is also possible that the model overestimates the link between the variations in transport of the Florida and Yucatan currents. We note, however, that the correlation between the transport time series shown in Figure 2a from the 1/12° Atlantic Ocean FLAME model is 0.8 and is also considerably higher than is found between the Canek and cable data sets. Only further detailed monitoring efforts, especially of the Yucatan Channel, which has been much less monitored than the Florida Current, will be able to clarify this issue.

[35] Evidence for the compensation effect is also provided by *Hamilton et al.* [2005]. They note that variations in the cable-estimated transport between Florida and the Bahamas are not necessarily an accurate indicator of the transport variability of the Loop Current as it exits the Gulf of Mexico (and by implication, the transport through the Yucatan Channel into the gulf), implying that in their opinion, significant transport must pass through the passageways north of Cuba and south of the cable site at 27°N. They base their conclusion on estimated transports from December 1990 to November 1991 based on moored arrays at several sections in the Straits of Florida extending both south and southeastward from Key West and between Florida and the Bahamas, including the side channels north of Cuba.

7. Summary and Discussion

[36] Using a number of different model experiments, we have examined the link between variations in the vertically integrated transport through the Yucatan Channel and the intrusion of the Loop Current into the Gulf of Mexico in association with ring shedding. Such transport variations are a feature of the 1/12° FLAME model of the Atlantic Ocean (Figure 2) and can also be seen in the model study of *Cherubin et al.* [2005]. We have seen that in the models the transport of the Yucatan Channel reaches a minimum when the Loop Current intrusion into the Gulf of Mexico is at a maximum, typically just prior to ring shedding. Likewise, the maximum transport through the Yucatan Channel occurs typically soon after a ring has been shed and is associated with a bulging of the Loop Current away from the northwest coast of Cuba, in contrast to the pinching of the Loop Current close to the coast when there is a strong intrusion into the gulf. We argued that the transport variations associated with the Loop Current intrusion arise from the interaction between the density anomalies associated with the Loop Current evolution and the variable bottom topography, the mechanism being the form drag effect across the ridge connecting Florida and Cuba. We have also argued

that transport variations through the Yucatan Channel are at least partly compensated by flow variations through the channels north of Cuba, notably the Old Bahama Channel (what we have called the compensation effect). Using a version of our model driven by 6 hourly wind stress derived from NCEP wind data, we showed that in addition to the influence of the Loop Current intrusion, the compensation effect also operates on time scales shorter than 30 days but in this case the dynamics are wind driven. We note that because of the compensation effect, transport through the Yucatan Channel and between Florida and the Bahamas (at the site of the submarine cable [*Baringer and Larsen*, 2001]) does not vary in unison in either our model or the FLAME model, although in both models the corresponding transport time series are highly correlated (greater than 0.8). This contrasts with the very low correlation (0.15) between the transport times series measured during the Canek program [*Sheinbaum et al.*, 2002] and the cable estimate [*Baringer and Larsen*, 2001]. It should be noted, however, that we have less than 1 year of data with which to compute the correlation of 0.15 and that 1 year is not long enough to allow sampling of the Loop Current intrusion events that dominate the model transport time series. Nevertheless, discrepancies of this kind argue the need for more detailed monitoring of the flow pathways entering and leaving the Gulf of Mexico and the Bahama Island chain.

[37] Clearly, an improvement in the model would be to replace the seasonally varying transport on the northern boundary by a more realistic representation of the daily transport variability. A more realistic specification of the time varying transport on the northern boundary would also shed light on the mechanisms governing the daily transport variability seen in the cable data (see *Greatbatch et al.* [1995], who noted the importance in their model of forcing north of the Florida Straits for driving Florida Current transport variability). Another topic we have not addressed is whether the transport variations we have discussed can feedback and influence the intrusion of the Loop Current. As noted in section 1, many authors have suggested that changes in the flow conditions through the Yucatan Channel (e.g., flow velocity and the vorticity distribution) might play a role in preconditioning Loop Current intrusion and ring shedding [e.g., *Sheinbaum et al.*, 2002; *Ezer et al.*, 2003; *Oey et al.*, 2005; *Oey*, 2004]. Clearly, further work is required on the general topic of Florida and Yucatan Current transport variability.

References

Abascal, A. J., J. Sheinbaum, J. Candela, J. Ochoa, and A. Badan (2003), Analysis of flow variability in the Yucatan Channel, *J. Geophys. Res.*, *108*(C12), 3381, doi:10.1029/2003JC001922.

Atkinson, L. P., T. Berger, P. Hamilton, E. Waddell, K. Leaman, and T. N. Lee (1995), Current meter observations in the Old Bahama Channel, *J. Geophys. Res.*, *100*, 8555–8560, doi:10.1029/95JC00586.

Baringer, M. O., and J. C. Larsen (2001), Sixteen years of Florida Current transport at 27°N, *Geophys. Res. Lett.*, *28*, 3179–3182, doi:10.1029/2001GL013246.

Barnier, B., L. Siefridt, and P. Marchesiello (1995), Thermal forcing for a global ocean circulation model using a three-year climatology of ECMWF analyses, *J. Mar. Syst.*, *6*, 363–380, doi:10.1016/0924-7963(94)00034-9.

Bunge, L., J. Ochoa, A. Badan, J. Candela, and J. Sheinbaum (2002), Deep flows in the Yucatan Channel and their relation to changes in the Loop Current extension, *J. Geophys. Res.*, *107*(C12), 3233, doi:10.1029/2001JC001256.

Candela, J., S. Tanahara, M. Crepon, B. Barnier, and J. Sheinbaum (2003), Yucatan Channel flow: Observations versus CLIPPER ATL6 and MERCATOR PAM models, *J. Geophys. Res.*, *108*(C12), 3385, doi:10.1029/2003JC001961.

Cherubin, L. M., W. Sturges, and E. P. Chassignet (2005), Deep flow variability in the vicinity of the Yucatan Straits from a high-resolution numerical simulation, *J. Geophys. Res.*, *110*, C04009, doi:10.1029/2004JC002280.

Cunningham, S. A., et al. (2007), Temporal variability of the Atlantic meridional overturning circulation at 26.5°N, *Science*, *317*, 935–938, doi:10.1126/science.1141304.

da Silva, A. M., , C. C. Young-Molling, and S. Levitus (Eds.) (1994), *Anomalies of Heat and Momentum Fluxes*, NOAA Atlas NESDIS, vol. 3, 413 pp., NOAA, Silver Spring, Md.

Dietrich, D. E. (1998), Application of a modified Arakawa 'a' grid ocean model having reduced numerical dispersion to the Gulf of Mexico circulation, *Dyn. Atmos. Oceans*, *27*, 201–217, doi:10.1016/S0377-0265(97)00009-2.

Dietrich, D. E., C. A. Lin, A. Mestas-Nunez, and D. S. Ko (1997), A high resolution numerical study of Gulf of Mexico fronts and eddies, *Meteorol. Atmos. Phys.*, *64*, 187–201, doi:10.1007/BF01029692.

Eden, C., R. J. Greatbatch, and J. Willebrand (2007), A diagnosis of thickness fluxes in an eddy-resolving model, *J. Phys. Oceanogr.*, *37*, 727–742, doi:10.1175/JPO2987.1.

Ezer, T., L.-Y. Oey, W. Sturges, and H.-C. Lee (2003), The variability of currents in the Yucatan Channel: Analysis of results from a numerical ocean model, *J. Geophys. Res.*, *108*(C1), 3012, doi:10.1029/2002JC001509.

Greatbatch, R. J., Y. Lu, B. deYoung, and J. Larsen (1995), The variation of transport through the Straits of Florida: A barotropic model study, *J. Phys. Oceanogr.*, *25*, 2726–2740, doi:10.1175/1520-0485(1995)025<2726:TVOTTT>2.0.CO;2.

Hamilton, P., J. C. Larsen, K. D. Leaman, T. N. Lee, and E. Waddell (2005), Transports through the Straits of Florida, *J. Phys. Oceanogr.*, *35*, 308–322, doi:10.1175/JPO-2688.1.

Hughes, C. W., and B. A. de Cuevas (2001), Why western boundary currents in realistic oceans are inviscid: A link between form stress and bottom pressure torques, *J. Phys. Oceanogr.*, *31*, 2871–2885, doi:10.1175/1520-0485(2001)031<2871:WWBCIR>2.0.CO;2.

Huh, O. K., W. J. Wiseman, and L. J. Rouse (1981), Intrusion of Loop Current waters onto the west Florida continental shelf, *J. Geophys. Res.*, *86*, 4186–4192, doi:10.1029/JC086iC05p04186.

Hurlburt, H. E., and J. D. Thompson (1980), A numerical study of Loop Current intrusions and eddy shedding, *J. Phys. Oceanogr.*, *10*, 1611–1651, doi:10.1175/1520-0485(1980)010<1611:ANSOLC>2.0.CO;2.

Johns, W. E., T. L. Townsend, D. M. Fratantoni, and W. D. Wilson (2002), On the Atlantic inflow to the Caribbean Sea, *Deep Sea Res., Part I*, *49*, 211–243, doi:10.1016/S0967-0637(01)00041-3.

Johns, W. E., R. H. Smith, E. M. Johns, and W. D. Wilson (2008), The Caribbean mass budget revisited, *Eos Trans. AGU*, *89*(23), Jt. Assem. Suppl., Abstract OS34A-03.

Kanzow, T., S. A. Cunningham, D. Rayner, J. J.-M. Hirschi, W. E. Johns, M. O. Baringer, H. L. Bryden, L. M. Beal, C. S. Meinen, and J. Marotzke (2007), Observed flow compensation associated with the MOC at 26.5°N in the Atlantic, *Science*, *317*, 938–941, doi:10.1126/science.1141293.

Large, W. G., and S. Pond (1981), Open ocean momentum flux measurements in moderate to strong winds, *J. Phys. Oceanogr.*, *11*, 324–336, doi:10.1175/1520-0485(1981)011<0324:OOMFMI>2.0.CO;2.

Large, W. G., J. C. McWilliams, and S. C. Doney (1994), Oceanic vertical mixing: A review and a model with a nonlocal boundary layer parameterization, *Rev. Geophys.*, *32*, 363–404, doi:10.1029/94RG01872.

Larsen, J. C. (1992), Transport and heat flux of the Florida Current at 27°N derived from cross-stream voltages and profiling data: Theory and observations, *Philos. Trans. R. Soc. London, Ser. A*, *338*, 169–236, doi:10.1098/rsta.1992.0007.

Leaman, K. D., P. S. Vertes, L. P. Atkinson, T. N. Lee, P. Hamilton, and E. Waddell (1995), Transport, potential vorticity, and current/temperature structure across Northwest Providence and Santaren channels and the

Florida Current off Cay Sal Bank, *J. Geophys. Res.*, *100*, 8561–8569, doi:10.1029/94JC01436.

Marchesiello, P., J. C. McWilliams, and A. Shchepetkin (2001), Open boundary conditions for long-term integration of regional oceanic models, *Ocean Modell.*, *3*, 1–20, doi:10.1016/S1463-5003(00)00013-5.

Maul, G. A., and F. M. Vukovich (1993), The relationship between variations in the Gulf of Mexico Loop Current and Straits of Florida volume transport, *J. Phys. Oceanogr.*, *23*, 785–796, doi:10.1175/1520-0485(1993)023<0785:TRBVIT>2.0.CO;2.

Maul, G. A., D. A. Mayer, and S. R. Baig (1985), Comparisons between a continuous 3-year current-meter observation at the sill of the Yucatan Strait, satellite measurements of gulf Loop Current area, and regional sea level, *J. Geophys. Res.*, *90*, 9089–9096, doi:10.1029/JC090iC05p09089.

Murphy, S. J., H. E. Hurlburt, and J. J. O'Brien (1999), The connectivity of eddy variability in the Caribbean Sea, the Gulf of Mexico, and the Atlantic Ocean, *J. Geophys. Res.*, *104*, 1431–1454, doi:10.1029/1998JC900010.

Nof, D. (2005), The momentum imbalance paradox revisited, *J. Phys. Oceanogr.*, *35*, 1928–1939, doi:10.1175/JPO2772.1.

Nof, D., and T. Pichevin (2001), The ballooning of outflows, *J. Phys. Oceanogr.*, *31*, 3045–3058, doi:10.1175/1520-0485(2001)031<3045:TBOO>2.0.CO;2.

Ochoa, J., J. Sheinbaum, A. Badan, J. Candela, and D. Wilson (2001), Geostrophy via potential vorticity inversion in the Yucatan Channel, *J. Mar. Res.*, *59*, 725–747, doi:10.1357/002224001762674917.

Oey, L.-Y. (2004), Vorticity flux in the Yucatan Channel and Loop Current eddy shedding in the Gulf of Mexico, *J. Geophys. Res.*, *109*, C10004, doi:10.1029/2004JC002400.

Oey, L.-Y., H. Lee, and W. J. Schmitz Jr. (2003), Effects of winds and Caribbean eddies on the frequency of Loop Current eddy shedding: A numerical model study, *J. Geophys. Res.*, *108*(C10), 3324, doi:10.1029/2002JC001698.

Oey, L.-Y., T. Ezer, and H.-C. Lee (2005), Loop Current, rings, and related circulation in the Gulf of Mexico: A review of numerical models and future challenges, in *Circulation in the Gulf of Mexico: Observations and Models*, *Geophys. Monogr. Ser.*, vol. 161, edited by W. Sturges and A. Lugo-Fernandez, pp. 31–56, AGU, Washington, D. C.

Orlanski, I. (1976), A simple boundary condition for unbounded hyperbolic flows, *J. Comput. Phys.*, *21*, 251–269, doi:10.1016/0021-9991(76)90023-1.

Pichevin, T., and D. Nof (1997), The momentum imbalance paradox, *Tellus, Ser. A*, *49*, 298–319, doi:10.1034/j.1600-0870.1997.t01-1-00009.x.

Schmitz, W. J., and P. L. Richardson (1991), On the sources of the Florida Current, *Deep Sea Res., Part A*, *32*, S379–S409.

Schmitz, W. J., Jr., J. D. Thompson, and J. R. Luyten (1992), Sverdrup circulation for the Atlantic along 24°N, *J. Geophys. Res.*, *97*, 7251–7256, doi:10.1029/92JC00417.

Schott, F., and R. Zantopp (1985), Florida Current: Seasonal and interannual variability, *Science*, *227*, 308–311, doi:10.1126/science.227.4684.308.

Sheinbaum, J., J. Candela, A. Badan, and J. Ochoa (2002), Flow structure and transport in the Yucatan Channel, *Geophys. Res. Lett.*, *29*(3), 1040, doi:10.1029/2001GL013990.

Sheng, J., and L. Tang (2003), A numerical study of circulation in the western Caribbean Sea, *J. Phys. Oceanogr.*, *33*, 2049–2069, doi:10.1175/1520-0485(2003)033<2049:ANSOCI>2.0.CO;2.

Sheng, J., and L. Tang (2004), A two-way nested-grid ocean-circulation model for the Meso-American Barrier Reef system, *Ocean Dyn.*, *54*, 232–242, doi:10.1007/s10236-003-0074-3.

Sheng, J., D. G. Wright, R. J. Greatbatch, and D. E. Dietrich (1998), CANDIE: A new version of the DieCAST ocean circulation model, *J. Atmos. Oceanic Technol.*, *15*, 1414–1432, doi:10.1175/1520-0426(1998)015<1414:CANVOT>2.0.CO;2.

Sheng, J., R. J. Greatbatch, and D. G. Wright (2001), Improving the utility of ocean circulation models through adjustment of the momentum balance, *J. Geophys. Res.*, *106*, 16,711–16,728, doi:10.1029/2000JC000680.

Smagorinsky, J. (1963), General circulation experiments with the primitive equations: I. The basic experiment, *Mon. Weather Rev.*, *91*, 99–164, doi:10.1175/1520-0493(1963)091<0099:GCEWTP>2.3.CO;2.

Sturges, W. (1992), The spectrum of Loop Current variability from gappy data, *J. Phys. Oceanogr.*, *22*, 1245–1256, doi:10.1175/1520-0485(1992)022<1245:TSOLCV>2.0.CO;2.

Sturges, W., and R. Leben (2000), Frequency of ring separations from the Loop Current in the Gulf of Mexico: A revised estimate, *J. Phys. Oceanogr.*, *30*, 1814–1819, doi:10.1175/1520-0485(2000)030<1814:FORSFT>2.0.CO;2.

Tang, L., J. Sheng, B. G. Hatcher, and P. F. Sale (2006), Numerical study of circulation, dispersion, and hydrodynamic connectivity of surface waters on the Belize shelf, *J. Geophys. Res.*, *111*, C01003, doi:10.1029/2005JC002930.

Thuburn, J. (1996), Multidimensional flux-limited advection schemes, *J. Comput. Phys.*, *123*, 74–83, doi:10.1006/jcph.1996.0006.

Vukovich, F. M. (1995), An updated evaluation of the Loop Current's eddy-shedding frequency, *J. Geophys. Res.*, *100*, 8655–8659, doi:10.1029/95JC00141.

Wiseman, W. J., Jr., and S. P. Dinnel (1988), Shelf currents near the mouth of the Mississippi River, *J. Phys. Oceanogr.*, *18*, 1287–1291, doi:10.1175/1520-0485(1988)018<1287:SCNTMO>2.0.CO;2.

––––––––––––––––––

R. J. Greatbatch, IFM-GEOMAR, Durstenbrooker Weg 20, D-24105 Kiel, Germany.

Y. Lin and J. Sheng, Department of Oceanography, Dalhousie University, 1355 Oxford Street, Halifax, NS B3H 4J1, Canada. (yuehua.lin@phys.ocean.dal.ca)